

## **Nonequilibrium Molecular Dynamics of Liquid Crystals<sup>1</sup>**

**S. S. Sarman,<sup>2,4</sup> P. T. Cummings,<sup>2,5</sup> and D. J. Evans<sup>6</sup>**

---

During the last 15 years, nonequilibrium molecular dynamics (NEMD) has been successfully applied to study transport phenomena in fluids that are isotropic at equilibrium. A natural extension is therefore to study liquid crystals, which are anisotropic at equilibrium. The lower symmetry of these systems means that the linear transport coefficients are considerably more complicated than in an isotropic system. Part of the reason for this is that there are cross-couplings between tensors of different rank and parity. Such couplings are symmetry-forbidden in isotropic phases. In this paper, we review some of fundamental theoretical results we have derived concerning the rheology of liquid crystals, report NEMD simulations of thermal conductivity and shear viscosity of liquid crystals, and present NEMD simulations of shear cessation phenomena. All of the NEMD results are presented for a model liquid crystal fluid which is a modification of the Gay-Berne fluid. The results obtained are in qualitative agreement with experimental measurements on liquid crystal systems.

---

**KEY WORDS:** liquid crystals; nematic phase; nonequilibrium molecular dynamics; planar Couette flows; rheology.

---

<sup>1</sup> Paper presented at the Twelfth Symposium on Thermophysical Properties, June 19–24, 1994, Boulder, Colorado, U.S.A.

<sup>2</sup> Department of Chemical Engineering, University of Virginia, Charlottesville, Virginia 22903-2442, U.S.A.

<sup>3</sup> Present address: Department of Chemical Engineering, University of Tennessee, Knoxville, Tennessee 37996-2200, U.S.A.

<sup>4</sup> Present address: Chemical Technology Division, Oak Ridge National Laboratory, Oak Ridge, Tennessee 37831-6181, U.S.A.

<sup>5</sup> To whom correspondence should be addressed.

<sup>6</sup> Research School of Chemistry, Australian National University, Canberra, ACT 0200, Australia.

## 1. INTRODUCTION

Transport properties of axially symmetric systems such as nematic liquid crystals are considerably more complicated than those of isotropic fluids. The thermal conductivity and the diffusion coefficient are second-rank tensors with two independent components. This anisotropy causes the director to align relative to a concentration or temperature gradient [1]. The viscosity is a fourth-rank tensor with seven independent components. Cross-couplings that are symmetry-forbidden in isotropic fluids are permitted in anisotropic fluids. In particular, one has a cross-coupling between the symmetric part of the strain rate and the antisymmetric part of the pressure tensor, and vice versa. This cross-coupling is responsible for alignment phenomena in liquid crystal flows.

Transport coefficients can be obtained either from the appropriate Green-Kubo relation, evaluated by conventional equilibrium molecular dynamics (EMD), or by nonequilibrium molecular dynamics (NEMD) methods [2]. In the latter case the system is coupled to a fictitious mechanical field. The field generates irreversible thermodynamic currents. The analytical expression for the field is chosen in such a way that the currents become the same as the ones induced by real Navier-Stokes forces. These forces include temperature, chemical potential, and velocity gradients. The transport coefficient in question is obtained as the ratio of the current to the field in the limit of zero field. The NEMD method also makes it possible to study how the thermodynamic currents affect the structure of the fluid. One can also study phenomena that occur far from equilibrium. One such phenomenon is shear cessation. If an isotropic fluid consisting of elongated molecules is subject to a high strain rate, a liquid-crystal-like phase will be induced. If the strain field is abruptly turned off, the shear stress will not immediately go to zero. There will be a residual stress that decays as the shear-induced liquid crystal phase reverts to the equilibrium isotropic phase.

In liquid crystals, many properties are best expressed relative to a director-based coordinate system. This is not a problem in the thermodynamic limit because in this case the director is virtually fixed. In a small system, such as a computer simulation cell, the director slowly diffuses on the unit sphere. In this case a director-based coordinate system is no longer an inertial frame. The drift of the director may also affect long-ranged time correlation functions and their time integrals, thus rendering the transport coefficients obtained from them incorrect. This problem can be solved by using a Gaussian constraint algorithm that fixes the orientation of the director. This technique has been successfully applied to the evaluation of the thermal conductivity of a nematic phase of the Gay-Berne fluid [1, 3].

The purpose of this paper is to demonstrate how various EMD and NEMD algorithms developed for isotropic fluids can be generalized to study transport properties of liquid crystals. The paper is organised as follows. In Section 2, we describe the model system. In Section 3, we review various NEMD algorithms and briefly discuss results obtained from them. Section 4 contains our conclusions.

**2. MODEL SYSTEM**

In most of the calculations reported in this article we have employed the Gay-Berne (GB) potential [3]. It can be regarded as a Lennard-Jones potential generalized to elliptical molecular cores. It has been shown to exhibit both nematic and smectic phases as well as ordinary isotropic phases [4]. The attractive part of the potential requires long cutoff radii in order to yield correct pressures, thus increasing the computation time. Therefore, we have chosen a purely repulsive variant of the GB potential,

$$U(\mathbf{r}_{12}, \hat{\mathbf{u}}_1, \hat{\mathbf{u}}_2) = 4\epsilon(\hat{\mathbf{r}}_{12}, \hat{\mathbf{u}}_1, \hat{\mathbf{u}}_2) \left[ \frac{\sigma_0}{r_{12} - \sigma(\hat{\mathbf{r}}_{12}, \hat{\mathbf{u}}_1, \hat{\mathbf{u}}_2) + \sigma_0} \right]^{18} \tag{1}$$

where  $\mathbf{r}_{12}$  is the distance vector from the center of mass of molecule 1 to the center of mass of molecule 2,  $\hat{\mathbf{r}}_{12}$  is the unit vector in the direction of  $\mathbf{r}_{12}$ ,  $r_{12}$  is the length of  $\mathbf{r}_{12}$ , and  $\hat{\mathbf{u}}_1$  and  $\hat{\mathbf{u}}_2$  are the unit vectors parallel to the axes of revolution. The parameter  $\sigma_0$  is of the length of the axis perpendicular to the axis of revolution. This is the minor axis of prolate ellipsoids and the major axis of oblate ellipsoids. The strength and range parameters  $\epsilon(\hat{\mathbf{r}}_{12}, \hat{\mathbf{u}}_1, \hat{\mathbf{u}}_2)$  and  $\sigma(\hat{\mathbf{r}}_{12}, \hat{\mathbf{u}}_1, \hat{\mathbf{u}}_2)$  are given by

$$\epsilon(\hat{\mathbf{r}}_{12}, \hat{\mathbf{u}}_1, \hat{\mathbf{u}}_2) = \epsilon_0 [1 - \chi^2 (\hat{\mathbf{u}}_1 \cdot \hat{\mathbf{u}}_2)^2]^{-1/2} \times \left\{ 1 - \frac{\chi'}{2} \left[ \frac{(\hat{\mathbf{r}}_{12} \cdot \hat{\mathbf{u}}_1 + \hat{\mathbf{r}}_{12} \cdot \hat{\mathbf{u}}_2)^2}{1 + \chi' \hat{\mathbf{u}}_1 \cdot \hat{\mathbf{u}}_2} + \frac{(\hat{\mathbf{r}}_{12} \cdot \hat{\mathbf{u}}_1 - \hat{\mathbf{r}}_{12} \cdot \hat{\mathbf{u}}_2)^2}{1 - \chi' \hat{\mathbf{u}}_1 \cdot \hat{\mathbf{u}}_2} \right] \right\}^2 \tag{2}$$

and

$$\sigma(\hat{\mathbf{r}}_{12}, \hat{\mathbf{u}}_1, \hat{\mathbf{u}}_2) = \sigma_0 \left\{ 1 - \frac{\chi'}{2} \left[ \frac{(\hat{\mathbf{r}}_{12} \cdot \hat{\mathbf{u}}_1 + \hat{\mathbf{r}}_{12} \cdot \hat{\mathbf{u}}_2)^2}{1 + \chi' \hat{\mathbf{u}}_1 \cdot \hat{\mathbf{u}}_2} + \frac{(\hat{\mathbf{r}}_{12} \cdot \hat{\mathbf{u}}_1 - \hat{\mathbf{r}}_{12} \cdot \hat{\mathbf{u}}_2)^2}{1 - \chi' \hat{\mathbf{u}}_1 \cdot \hat{\mathbf{u}}_2} \right] \right\}^{1/2} \tag{3}$$

The parameter  $\chi = (\kappa^2 - 1)/(\kappa^2 + 1)$ , where  $\kappa$  is the ratio of the axis of revolution and the axis perpendicular to the axis of revolution and  $\chi' = (\kappa'^2 - 1)/(\kappa'^2 + 1)$ , where  $\kappa'$  is the ratio of the potential energy minima of the side-to-side and the end-to-end configurations. The depth of

the potential minimum is given by  $\epsilon_0$ . Note that we use purely repulsive potentials, so there are no potential minima. However, we keep the values of  $\kappa'$ ,  $\chi'$ , and  $\epsilon_0$  used by previous authors [4].

We have been concerned with mainly prolate ellipsoids. The simulations were performed with 256 molecules with parameters  $\kappa = 3$  and  $\kappa' = 5$ . The cutoff radius beyond which the interaction forces and energies are zero is  $1.5\sigma(\hat{\mathbf{r}}_{12} \cdot \hat{\mathbf{u}}_1 \cdot \hat{\mathbf{u}}_2)$  and is thus orientation dependent. The reduced temperatures and densities,  $k_B T/\epsilon_0$  and  $n\sigma_0^3$ , have been set equal to 1.00 and 0.300, respectively. The whole  $k_B T/\epsilon_0 = 1.00$  isotherm can be found in Ref. 5. At low densities the fluid is isotropic. At approximately  $n\sigma_0^3 = 0.27$  there is a transition to a nematic phase.

The numerical results are expressed in length, time, and energy units of  $\sigma_0$ ,  $\tau = \sigma_0(m/\epsilon_0)^{1/2}$ , and  $\epsilon_0$ , respectively. The moments of inertia around the two axes perpendicular to the axis of revolution have both been given the value  $I = m\sigma_0^2$ , i.e., unity in reduced units. The equations of motion have been integrated by a fourth-order Gear predictor-corrector method with a time step of  $0.001\tau$  and Lee's Edwards' sliding-brick boundary conditions in the case of shear flow and with octahedral boundary conditions otherwise. Expressions for the forces and torques are given in Ref. 6.

### 3. THEORY

The degree of ordering in a liquid crystal is given by the scalar order parameter  $S$ , which is the largest eigenvalue of the symmetric traceless order tensor  $\mathbf{Q}$  given by

$$\mathbf{Q} = \frac{3}{2} \left[ \frac{1}{N} \sum_{i=1}^N \hat{\mathbf{u}}_i \hat{\mathbf{u}}_i - \frac{1}{3} \mathbf{1} \right] \quad (4)$$

where  $\mathbf{1}$  is the unit second-rank tensor. When the molecules are perfectly aligned, the order parameter is unity, and when the orientation is random the order parameter is zero. The unit eigenvector corresponding to the largest eigenvalue is called the director,  $\mathbf{n}$ . It is a measure of the average orientation of the system.

#### 3.1. Thermal Conductivity

In an axially symmetric system the thermal conductivity tensor is a second-rank tensor with two independent components relating the heat flow and the temperature gradient:  $\lambda_{\parallel\parallel}$  parallel to the director and  $\lambda_{\perp\perp}$  perpendicular to the director. The generalised Fourier's law is given by

$$\langle \mathbf{J}_Q \rangle = - [\lambda_{\parallel\parallel} \mathbf{nm} + \lambda_{\perp\perp} (\mathbf{1} - \mathbf{nm})] \cdot \nabla T \quad (5)$$

where  $\langle \mathbf{J}_Q \rangle$  is the macroscopic heat flux vector and  $T$  is the absolute temperature. It is assumed that the whole system remains in the same phase. The entropy production per unit volume and time,  $\sigma$ , due to heat conduction is

$$\sigma = -\frac{\langle \mathbf{J}_Q \rangle \cdot \nabla T}{T^2} = \frac{1}{T^2} [\lambda_{\perp\perp} \nabla T \cdot \nabla T + (\lambda_{\parallel\parallel} - \lambda_{\perp\perp})(\mathbf{n} \cdot \nabla T)^2] \quad (6)$$

Note that  $\sigma$  is orientation-dependent in anisotropic system. If  $\lambda_{\parallel\parallel} > \lambda_{\perp\perp}$ , the entropy production is minimal when the director is perpendicular to the temperature gradient. If  $\lambda_{\parallel\parallel} < \lambda_{\perp\perp}$ , a parallel orientation minimises  $\sigma$ . It is straightforward to derive Green-Kubo relations for the thermal conductivity,

$$\lambda_{zx} = \frac{V}{k_B T^2} \int_0^\tau dt \langle J_{Qz}(t) J_{Qz}(0) \rangle \quad (7)$$

where  $k_B$  is Boltzmann's constant,  $V$  is the volume,  $J_{Qz}(t)$  is the heat flux vector in the  $x$ -direction, and  $z = \parallel$  or  $\perp$ . The current  $\mathbf{J}_Q(t)$  is resolved in components parallel to the director,  $\mathbf{J}_{Q\parallel}(t) = \mathbf{J}_Q(t) \cdot \mathbf{nm}$ , and perpendicular to the director,  $\mathbf{J}_{Q\perp}(t) = \mathbf{J}_Q(t) - \mathbf{J}_{Q\parallel}(t)$ .

The thermal conductivity can also be obtained by a generalization of the Evans heat flow algorithm to molecular fluids [7]. The heat flux vector for a fluid consisting of rigid molecules is

$$\begin{aligned} V \mathbf{J}_Q = & \frac{1}{2} \sum_{i=1}^N \frac{\mathbf{p}_i}{m} \left( \frac{\mathbf{p}_i^2}{m} + \omega_{pi} \cdot \mathbf{I}_p \cdot \omega_{pi} + \sum_{j=1}^N \Phi_{ij} \right) \\ & - \frac{1}{2} \sum_{i=1}^N \sum_{j=1}^N \mathbf{r}_{ij} \left( \frac{\mathbf{p}_j}{m} \cdot \mathbf{F}_{ij} + \omega_{pi} \cdot \Gamma_{pij} \right) \end{aligned} \quad (8)$$

where  $m$  is the molecular mass and  $\mathbf{p}_i$  is the momentum. The principal angular velocity and inertia tensor are  $\omega_{pi}$  and  $\mathbf{I}_p$ ; hence the subscript  $p$ . The force and principal torque on particle  $i$  due to particle  $j$  are  $\mathbf{F}_{ij}$  and  $\Gamma_{pij}$ . A synthetic heat flow algorithm is

$$\dot{\mathbf{r}}_i = \frac{\mathbf{p}_i}{m} \quad (9)$$

$$\dot{\mathbf{p}}_i = \mathbf{F}_i + \left( \mathbf{S}_i - \frac{1}{N} \sum_{i=1}^N \mathbf{S}_i \right) \cdot \mathbf{F}_Q - \alpha \mathbf{p}_i \quad (10)$$

$$I \dot{\omega}_{pi} = \Gamma_{pi} - \frac{1}{2} \sum_{i=1}^N \Gamma_{pij} \mathbf{r}_{ij} \cdot \mathbf{F}_Q \quad (11)$$

where  $\mathbf{r}_i$  is the position of particle  $i$ ,  $\mathbf{F}_Q$  is the heat field, and

$$\mathbf{S}_i = \frac{1}{2} \left( \frac{\mathbf{p}_i^2}{m} + \boldsymbol{\omega}_{pi} \cdot \mathbf{I}_p \cdot \boldsymbol{\omega}_{pi} + \sum_{j=1}^N \Phi_{ij} \right) - \frac{1}{2} \sum_{j=1}^N \mathbf{r}_{ij} \mathbf{F}_{ij} \quad (12)$$

The omitted equation relating  $d\hat{\mathbf{u}}_i/dt$  and  $\omega_i$  is expressed in terms of quaternions [8]. The multiplier  $\alpha$  is determined by requiring that the translation kinetic energy should be a constant of motion [1]. From these equations of motion and linear response theory, one gets the following expression for the thermal conductivity:

$$\lambda_{zz} = \lim_{F_Q \rightarrow 0} M_{zz}(F_Q) = \lim_{F_Q \rightarrow 0} \lim_{t \rightarrow \infty} \frac{\langle J_{Qz}(t) \rangle}{TF_{Qz}} \quad (13)$$

This algorithm has been applied to calculate the thermal conductivity of various phases of the Gay-Berne fluid. In general, not unexpectedly, one can say that the thermal conductivity is about two or three times as large in the parallel direction as in the perpendicular direction in a prolate ellipsoid fluid. The reverse is true for oblate ellipsoids. Equilibrium Green-Kubo methods and NEMD algorithms give consistent results. An interesting phenomenon that occurs in liquid crystals subject to heat flow is that there is a preferred orientation of the director relative to the temperature gradient. In a nematic liquid crystal consisting of prolate ellipsoids,  $\lambda_{\parallel\parallel} > \lambda_{\perp\perp}$ ; and the director prefers to be perpendicular to the temperature gradient. In a fluid consisting of oblate ellipsoids,  $\lambda_{\parallel\parallel} < \lambda_{\perp\perp}$ , and the director prefers the parallel orientation. This behavior can be rationalized by analyzing the expression for the entropy production, Eq. 6. In both cases the director alignment minimizes the dissipation [1].

### 3.2. Director Constraint Algorithm

Many properties are best expressed relative to a director-based coordinate system. This is not a problem in the thermodynamic limit because in an infinite system the director is virtually fixed. However, in a small system such as a simulation cell, the director is slowly diffusing on the unit sphere. This means that a director-based coordinate system is no longer an inertial frame. The tails of the time correlation functions will also be affected by the rotational diffusion of the director. The transport coefficients obtained from the correlation functions will thus be incorrect. We solve this problem by augmenting the equations for the angular accelerations by two constraint torques [1],

$$I\dot{\boldsymbol{\omega}}_i = \boldsymbol{\Gamma}_i + I\dot{\lambda}_x \frac{\partial \Omega_x}{\partial \boldsymbol{\omega}_i} + I\dot{\lambda}_y \frac{\partial \Omega_y}{\partial \boldsymbol{\omega}_i} \quad (14)$$

where  $\Omega_x$  and  $\Omega_y$  are two components of the angular velocity of the director. It is possible to find expressions for the multipliers  $\lambda_x$  and  $\lambda_y$  in terms of phase variables in such a way that the director becomes fixed. However, these expressions are very complicated and are omitted. One can show that these constraint equations do not cause any additional dissipation when the director is fixed. This makes it possible to prove rigorously that the constraint equations do not affect ensemble averages of phase functions or time correlation functions.

Numerical tests of this algorithm have shown that it works very well. If one constrains the director to point in the  $z$ -direction (i.e.,  $n_z = 1$ ),  $n_x$  and  $n_y$  never exceed  $10^{-8}$ . The dissipation induced by the constraint torques, which should be exactly zero, never exceeds  $10^{-7}$  in reduced units. This algorithm is consequently a very powerful tool to use in liquid-crystal simulations.

### 3.3. Newtonian Shear Flow

Another important nonequilibrium system is a fluid subject to a Couette strain field. This system can be exactly modeled by applying the isokinetics SLLOD [2] equations of motion for a molecular fluid [11],

$$\dot{\mathbf{r}}_i = \frac{\mathbf{p}_i}{m} + \mathbf{e}_x \gamma y_i \tag{15a}$$

$$\dot{\mathbf{p}} = \mathbf{F}_i - \mathbf{e}_x \gamma p_{yi} - \alpha \mathbf{p}_i \tag{15b}$$

where  $\mathbf{e}_x$  is the unit vector in the  $x$  direction and  $\gamma = \partial u_x / \partial y$  is the velocity gradient. If the Reynolds number is low, the streaming velocity at the center of mass of particle  $i$  is  $\gamma y_i$ , so the peculiar velocity of the center of mass of the particle is  $p_i/m$ . The Gaussian multiplier  $\alpha$  is determined by making the peculiar kinetic energy a constant of motion,

$$\alpha = \frac{\sum_{i=1}^N [\mathbf{F}_i \cdot \mathbf{p}_i - \gamma p_{xi} p_{yi}]}{\sum_{i=1}^N \mathbf{p}_i^2} \tag{16}$$

Note that this thermostat does not exert any torque on the molecules or the director and it consequently does not affect the shear-induced alignment.

The viscosity of a nematic liquid crystal is a fourth-rank tensor with seven independent components. The definitions and the Green-Kubo relations for these elements are straightforward but very tedious to define and are reported elsewhere [12]. However, one often defines three effective viscosities, the Miesowicz viscosities [9],  $\langle p_{yx} \rangle = \eta_i \gamma$ , with the director

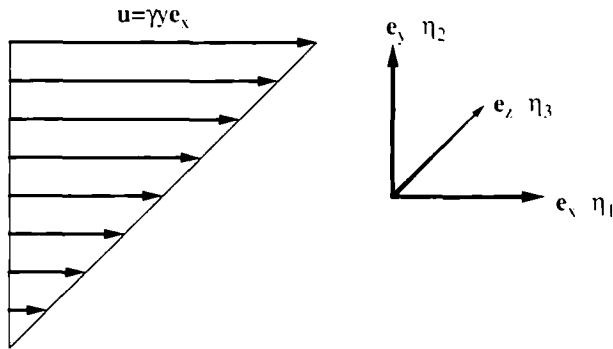


**Fig. 1.** Definitions of the Miesowicz viscosities. We assume that the stream lines are parallel to the  $e_x$  direction and the velocity varies linearly in the  $e_y$  direction. The shear plane is defined as the  $xy$  plane. The viscosity coefficient  $\eta_1$  is the ratio  $-\langle p_{yx} \rangle / \dot{\gamma}$ ; when the director is parallel to the stream lines;  $\eta_2$  is this ratio when the director is perpendicular to the stream lines and lies in the shear plane. Finally,  $\eta_3$  is the effective viscosity when the director is perpendicular to the stream lines and normal to the shear plane.

oriented in turn in the  $x$ ,  $y$ , and  $z$  directions; see Fig. 1. In experimental measurements the director is oriented by applying a magnetic field. In computer simulations of liquid-crystal model systems, it is very convenient to use our director-constraint method. We can fix the director in any direction and calculate the shear stress.

We have calculated the Miesowicz viscosities for two reduced strain rates, 0.02 and 0.04. The results are shown in Table I. As one can see,  $\eta_2$  is much larger than  $\eta_3$ , which is larger than  $\eta_1$ . Similar ratios of the Miesowicz viscosities have been found experimentally. It is easy to realize that  $\eta_1$  must be the smallest viscosity, because when the prolate molecules are parallel to the stream lines the molecule can slide past each other very easily.

**Table I.** The Miesowicz Viscosities as Functions of the Strain Rate

$\dot{\gamma}$	$\eta_1$	$\eta_2$	$\eta_3$
0.02	$0.86 \pm 0.1$	$15.0 \pm 0.1$	$2.62 \pm 0.1$
0.04	$0.87 \pm 0.1$	$14.4 \pm 0.1$	$2.58 \pm 0.02$



### 3.4. Nonlinear Flow Phenomena

So far we have dealt mostly with linear transport processes, i.e., where there is a linear relation between thermodynamic forces and fluxes. However, there is a wide range of interesting nonlinear flow phenomena in liquid crystals. One of them is shear-induced ordering. If a fluid consisting of rod-like molecules is subject to a weak Couette strain field, the molecules will be aligned. In the linear regime the alignment angle is equal to  $45^\circ$  relative to the stream lines. The order parameter is proportional to the strain rate, so if the strain rate is not very high, the fluid remains isotropic. As the strain rate increases the order parameter increases and one breaks the symmetry of the system. One can consequently turn an isotropic fluid consisting of elongated molecules into a nematic liquid crystal by applying a strong strain rate. This is a well-known phenomenon and it has been observed in a wide variety of liquid model systems such as diatomics, the Gay-Berne fluid, and various alkane models [10].

When the strain rate is high enough the linear relation between the pressure tensor and the strain rate breaks down. The fluid consequently becomes non-Newtonian. One manifestation of this is that the stress response to the strain rate is no longer instantaneous. If the strain rate changes, the pressure tensor will not be proportional to the strain rate, as it is in the Newtonian regime. If there is a step increase in the strain rate, there will be stress

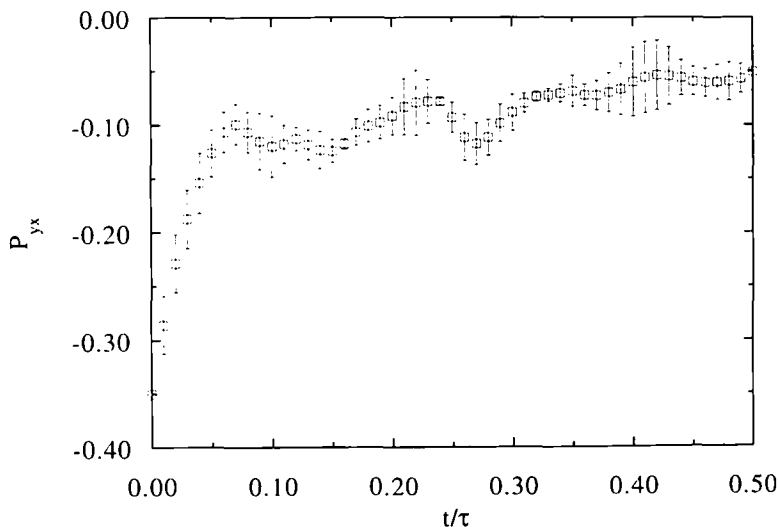


Fig. 2. The transient response of  $P_{yx}$ , the  $yx$  component of the pressure tensor, as a function of time immediately following shear cessation. That is,  $\gamma^* = \gamma\sigma_0(m/\epsilon_0)^{1/2} = 1.00$  for  $t < 0$  and  $\gamma^* = 0$  for  $t > 0$ .

overshoot. If the strain rate is abruptly turned off (shear cessation), the shear stress does not immediately go to zero as it would for a Newtonian fluid. We have studied how a Gay-Berne fluid behaves when a strong strain rate is instantaneously turned off. The results are shown in Fig. 2. As one can see there are two relaxation times. The first one is due to relaxation of the strain immediately following the cessation of the strain rate. This relaxation is very fast, almost-instantaneous as is seen in liquid-crystal solutions in a Newtonian solvent [13]. The second relaxation time is much longer than the first one and corresponds to the slow relaxation as the nematic phase, which is no longer stabilized by the strain field, breaks up and becomes isotropic. During this time there is some residual stress that decays to zero as the order parameter goes to zero.

#### 4. CONCLUSIONS

We have illustrated some of the peculiarities of the Newtonian and non-Newtonian rheology of liquid crystals and have demonstrated that equilibrium and nonequilibrium molecular dynamics simulations provide convenient and powerful methods for studying the molecular basis for liquid-crystalline behavior.

#### ACKNOWLEDGMENT

P.T.C. and S.S.S. gratefully acknowledge the support of this research by the National Science Foundation through Grant CTS-910136.

#### REFERENCES

1. S. Sarman, *J. Chem. Phys.* (in press).
2. D. J. Evans and G. P. Morriss, *Statistical Mechanics of Nonequilibrium Liquids* (Academic Press, London, 1990).
3. J. G. Gay and B. J. Berne, *J. Chem. Phys.* **74**:3316 (1981).
4. E. de Miguel, L. F. Rull, M. K. Chalam, K. E. Gubbins, and F. van Swol, *Mol. Phys.* **72**:593 (1991); E. de Miguel, L. F. Rull, M. K. Chalam, and K. E. Gubbins, *Mol. Phys.* **71**:1223, (1990); *Mol. Phys.* **74**:405 (1991).
5. S. Sarman and D. J. Evans, *J. Chem. Phys.* **99**:9021 (1993).
6. S. Sarman and D. J. Evans, *J. Chem. Phys.* **99**:620 (1993).
7. D. J. Evans and S. Murad, *Mol. Phys.* **68**:1219 (1989).
8. D. J. Evans, *Mol. Phys.* **34**:317 (1977).
9. P. G. deGennes, *The Physics of Liquid Crystals* (Clarendon Press, Oxford 1994); S. Hess, *J. Non-Equil. Thermodyn.* **11**:175 (1986).
10. S. Sarman, P. J. Daivis, and D. J. Evans, *Phys. Rev. E* **47**:1784 (1993).
11. P. T. Cummings and D. J. Evans, *J. Ind. Eng. Chem. Res.* **31**:1237 (1992).
12. S. Sarman, *J. Chem. Phys.* (1994), in preparation.
13. R. B. Bird, C. F. Curtiss, R. C. Armstrong, and O. Hassager, *Dynamics of Polymeric Liquids: Kinetic Theory*, 2nd ed. (John Wiley and Sons, New York, 1987), Vol. 2.